

# Photoelectron spectroscopy of nickel group dimers: Ni<sub>2</sub><sup>-</sup>, Pd<sub>2</sub><sup>-</sup>, and Pt<sub>2</sub><sup>-</sup>

Joe Ho,<sup>a)</sup> Mark L. Polak,<sup>b)</sup> Kent M. Ervin,<sup>c)</sup> and W. C. Lineberger

Department of Chemistry and Biochemistry, University of Colorado, and Joint Institute for Laboratory Astrophysics, University of Colorado and National Institute of Standards and Technology, Boulder, Colorado 80309-0440

(Received 24 June 1993; accepted 13 August 1993)

Negative ion photoelectron spectra of Ni<sub>2</sub><sup>-</sup>, Pd<sub>2</sub><sup>-</sup>, and Pt<sub>2</sub><sup>-</sup> are presented for electron binding energies up to 3.35 eV at an instrumental resolution of 8–10 meV. The metal cluster anions are prepared in a flowing afterglow ion source. Each dimer exhibits multiple low-lying electronic states and a vibrationally resolved ground state transition. Franck–Condon analyses yield the anion and neutral vibrational frequencies and the bond length changes between anion and neutral. The electron affinities are determined to be EA(Ni<sub>2</sub>)=0.926±0.010 eV, EA(Pd<sub>2</sub>)=1.685±0.008 eV, and EA(Pt<sub>2</sub>)=1.898±0.008 eV. The electronic configurations of the ground states are tentatively assigned. Comparison of the nickel group dimers to the coinage metal dimers sheds light on the *d* orbital contribution to the metal bonding in the nickel group dimers.

## I. INTRODUCTION

Spectroscopic study of the nickel group dimers has greatly enhanced our understanding of electronic structure and chemical bonding in transition metal dimers and small clusters in recent years. These dimers (Ni<sub>2</sub>, Pd<sub>2</sub>, and Pt<sub>2</sub>) are relatively simple compared to other transition metal dimers, since there are only one or two *d* holes (Ni and Pt), or a fully filled *d* shell (Pd) in the ground electronic configuration of the constituent atoms. The bonding behavior of these dimers should be similar to the neighboring coinage metal dimers in that the interactions of the *s* electrons dominate the bonding and the electronic structure of the dimers. However, since the *s* and *d* orbitals have similar energies, the *d* electrons may participate in the bonding as well.<sup>1</sup> By comparing bonding properties between the nickel group and the coinage metal dimers, we can obtain insight into the participation of *d* electrons in metal bonding.<sup>2</sup> Therefore, the nickel group dimers can serve as a starting point for systematic studies of open *d*-shell transition metal dimers.

Ni<sub>2</sub> has been the subject of a large number of *ab initio* calculations. An early extended Hückel calculation<sup>3</sup> predicts the ground state to be <sup>3</sup>Σ<sub>g</sub><sup>-</sup>, with *D*<sub>e</sub>=2.78 eV and *r*<sub>e</sub>=2.21 Å. Using local spin density theory, Harris and Jones predicted<sup>4</sup> the same <sup>3</sup>Σ<sub>g</sub><sup>-</sup> ground state, with *D*<sub>e</sub>=2.70 eV, *r*<sub>e</sub>=2.18 Å, and ω<sub>e</sub>=320 cm<sup>-1</sup>. Most of the reports of Ni<sub>2</sub> have involved Hartree–Fock configuration interaction methods, and agreement among these calculations is reasonably good.<sup>5</sup> It is agreed that the bonding consists of a (4*s*<sub>g</sub>)<sup>2</sup> bond with a weakly interacting 3*d*<sup>18</sup> “core,” and the 3*d* holes are preferentially placed in δ orbitals, resulting in <sup>3</sup>Σ<sub>u</sub><sup>+</sup>, <sup>3</sup>Σ<sub>g</sub><sup>-</sup>, <sup>1</sup>Σ<sub>g</sub><sup>+</sup>, <sup>1</sup>Σ<sub>u</sub><sup>-</sup>, <sup>3</sup>Γ<sub>u</sub>, and <sup>1</sup>Γ<sub>g</sub> molecular states

which are nearly degenerate so long as spin–orbit interactions are neglected. Lying about 0.25 eV above these lowest states are the terms arising from a πδ-hole configuration, followed by the other configurations. A restricted Hartree–Fock calculation found<sup>6</sup> *r*<sub>e</sub>=2.28 Å and ω<sub>e</sub>=240 cm<sup>-1</sup>. Very recently, Spain and Morse<sup>7</sup> have applied ligand field theory to the low lying electronic structure of Ni<sub>2</sub>, and found significant spin–orbit mixing between some states of δδ- and πδ-hole configurations. This mixing is found to spread out the first-order nearly degenerate δδ-hole states over about 800 cm<sup>-1</sup>.

In experimental studies, several transitions have been observed in absorption spectra of Ni<sub>2</sub> deposited in rare gas matrices.<sup>1</sup> Devore *et al.*<sup>8</sup> observed a series of sharp absorptions with ν<sub>00</sub>=21 786 cm<sup>-1</sup> and ω'<sub>e</sub>=192 cm<sup>-1</sup>. Moskovits and Hulse<sup>9</sup> found two discrete bands at 18 920 and 26 500 cm<sup>-1</sup>, and a continuous band peaking at 24 000 cm<sup>-1</sup>. Ahmed and Nixon<sup>10</sup> observed an emission band system with ν<sub>00</sub>=22 246 cm<sup>-1</sup>, ω<sub>e</sub>=380.95 cm<sup>-1</sup>, and ω<sub>e</sub>x<sub>e</sub>=1.08 cm<sup>-1</sup> for the lower electronic state. The gas phase Ni<sub>2</sub> electronic spectrum has been reported by Morse *et al.*<sup>11</sup> using a resonant two photon ionization technique. No transitions could be detected corresponding to the band systems observed in rare gas matrices. An abrupt onset of complicated spectral structure and a sharp transition from long (≈10 μs) to short (≈10 ns) lifetimes were observed at 16 680 cm<sup>-1</sup>, which is interpreted<sup>11</sup> to represent the adiabatic dissociation limit of *D*<sub>0</sub>=2.068±0.01 eV. The isolated vibronic bands observed near 8500 Å established a bond length of the lower state of the transition as 2.200±0.007 Å, and the transition was assigned to Ω'=5←Ω''=4. The authors tentatively assigned the lower state to be either a <sup>1</sup>Γ<sub>g</sub> or <sup>3</sup>Γ<sub>u</sub> electronic term. In work still in progress, Morse and co-workers<sup>12</sup> have found that improved cooling suppresses transitions arising from the Ω=4 state. Upon cooling, the remaining transitions are from an Ω=0 state with *r*=2.155±0.001 Å, which is very likely the ground state. The parity of the Ω=0 state was not determined, but the state should<sup>7</sup> arise either from a

<sup>a)</sup>Present address: Chemistry Division, Argonne National Laboratory, Argonne, Illinois 60439.

<sup>b)</sup>Present address: Aerospace Corporation, P.O. Box 92957, M.S. M5/747, El Segundo, California 90245-4691.

<sup>c)</sup>Present address: Department of Chemistry, University of Nevada, Reno, Nevada 89557.

mixture of the  $^1\Sigma_u^-$  and  $^3\Sigma_u^+$  states or from a mixture of the  $^1\Sigma_g^+$  and  $^3\Sigma_g^-$  states, all of which are associated with a  $\delta\delta$ -hole configuration.

The theoretical study of  $\text{Pt}_2$  is quite interesting because it provides a wealth of information regarding the question of  $d$  orbital participation in bonding. Basch *et al.*<sup>13</sup> used a bonding-pair correlated self-consistent field (SCF) calculation to study low-lying  $\text{Pt}_2$  electronic states. Although considering only four representative  $\delta\delta$ - and  $\sigma\sigma$ -hole states, the investigation provides preliminary insight into the electronic states. Balasubramanian<sup>14</sup> carried out a size consistent complete active space MCSCF (CASSCF) calculation, followed by first-order configuration interaction calculations on the low-lying electronic states of  $\text{Pt}_2$ . Introducing the spin-orbit interaction through a relativistic configuration interaction, he studied the electronic ground and 21 low-lying excited states, and calculated the molecular parameters for these states.

Few experimental data have been reported on  $\text{Pt}_2$ . Gupta *et al.*<sup>15</sup> have detected  $\text{Pt}_2$  in equilibrium with Pt at high temperature. Assuming a  $^1\Sigma$  ground state, they obtained  $D_0=3.71\pm 0.16$  eV. Jasson and Scullman<sup>16</sup> have studied  $\text{Pt}_2$  in an argon matrix. In the  $11\,250\text{ cm}^{-1}$  region, they found an excited state with a  $217\text{ cm}^{-1}$  vibrational frequency. The gas phase  $\text{Pt}_2$  optical spectrum has been investigated by Taylor *et al.*<sup>17</sup> using resonant two photon ionization spectroscopy. In the region of  $11\,300\text{--}26\,300\text{ cm}^{-1}$ , numerous vibronic bands are observed and 26 excited states have been characterized. They obtained  $D_0=3.14\pm 0.02$  eV based on the observed onset of predissociation, a value considerably smaller than that reported by Gupta *et al.*

Theoretical investigations of  $\text{Pd}_2$  at a variety of levels have been carried out.<sup>13,18–20</sup> Basch *et al.*<sup>13</sup> used a relativistic effective core potential (ECP) and a limited multiconfiguration self-consistent field (MCSCF) method; Shim and Gingerich<sup>18</sup> employed a nonrelativistic all-electron Hartree-Fock (HF)/valence configuration interaction (CI) calculation; and Salahub<sup>19</sup> applied model-potential methods with relativistic corrections. All of the studies have demonstrated the complexity of the  $\text{Pd}_2$  electronic structure, but they vary with respect to the ground state assignments and the energies of the many low-lying electronic states.<sup>1</sup> Balasubramanian<sup>20</sup> recently carried out complete active space self-consistent field (CASSCF) calculations followed by multireference singles and doubles CI (MRSDCI) and relativistic CI, to determine the low-lying electronic states. This calculation, utilizing the largest basis set to date and a spin-orbit perturbation correction, included 41 electronic states below  $9000\text{ cm}^{-1}$ . A  $^3\Sigma_u^+(1_u)$  ground state and its corresponding antiparallel spin coupling state  $^1\Sigma_u^+$  at  $4443\text{ cm}^{-1}$  are among the relevant predictions. Lee *et al.*<sup>21</sup> calculated spectroscopic parameters of  $\text{Pd}_2$  using local-spin-density (LSD) theory and a full relativistic norm-conserving pseudopotential; they predicted a  $^3\Sigma_u^+$  ground state with a vibrational frequency of  $222\text{ cm}^{-1}$ .

Again, experimental data for  $\text{Pd}_2^-$  are scarce. High temperature measurements using Knudsen cell effusion

mass spectrometry<sup>22</sup> have a second-law value of  $D_0(\text{Pd}_2)=1.13\pm 0.22$  eV. Coupled with *ab initio* calculations, a reanalysis<sup>18</sup> of these data provide a third-law value of  $D_0(\text{Pd}_2)=1.03\pm 0.16$  eV. The Morse group attempted two-photon ionization spectroscopy of gas phase  $\text{Pd}_2$ , but no transitions were observed in their scanning range.<sup>23</sup> To our knowledge, no other gas-phase spectroscopic studies on  $\text{Pd}_2$  have been reported.

In this paper, the ultraviolet (351.1 nm) photoelectron spectra of the nickel group dimer anions  $\text{Ni}_2^-$ ,  $\text{Pd}_2^-$ , and  $\text{Pt}_2^-$  are presented. Experimental spectra are presented in Sec. III. Franck-Condon analyses yield vibrational constants and bond length changes, along with determinations of electron affinities. The anion dissociation energies are also calculated. The anion and neutral ground states and their electronic configurations are tentatively assigned. Since photoelectron spectra of  $\text{Pd}_2^-$  have been reported,<sup>24</sup> the pertinent results will be only briefly summarized for comparison with  $\text{Ni}_2^-$  and  $\text{Pt}_2^-$ . In the discussion, comparison of *ab initio* calculations to our experimental results shows relatively good agreement, considering the difficulty of the calculations associated with these complex systems. We also compare the nickel and coinage metal dimers, and explore the level of  $d$  electron participation in transition metal cluster bonding. Since the palladium dimers exhibit anomalous behavior, the following discussion is in the order Ni, Pt, and Pd rather than the normal periodic order.

## II. EXPERIMENTAL METHOD

The negative ion photoelectron spectrometer and metal cluster anion source have already been described in detail.<sup>25–27</sup> Here, we will briefly describe the metal ion production. The metal cluster anions are produced in a flowing afterglow ion source by cathodic sputtering with a dc discharge. A mixture of 10%–20% argon (ultrahigh purity) in helium (99.999%) flows over the metal cathode. The cathode is fabricated from high purity (>99.9%) nickel, palladium, or platinum metals. The cathode is negatively biased, typically at 3–5 kV with respect to the ground, producing a 10–30 mA discharge. The dimer anion is invariably the least intense small ( $\leq 6$  atoms) cluster, but currents of 0.5–4 pA of  $\text{Ni}_2^-$ ,  $\text{Pd}_2^-$ , and  $\text{Pt}_2^-$  can be obtained.

The absolute electron kinetic energy for the photoelectron spectra is calibrated against the precisely known electron affinities of O and the metal atoms, Ni, Pd, and Pt.<sup>28</sup> Spectra are corrected for an energy scale compression factor, calibrated on the known energy level spacings of the tungsten atom, or the Ni, Pd, and Pt atoms.<sup>29</sup> The instrumental resolution of the spectrometer is determined by the linewidth of an isolated atomic transition to be 8–10 meV. Because the nickel group metals react readily with oxygen, the three dimer anions are relatively difficult to produce with the cathode discharge ion source, and they are usually accompanied by various metal oxides, despite attempts to minimize oxygen contamination in the system. Although the mass resolution of the Wien filter is adequate to separate all three dimers from their oxides, the metal oxides

can be much more abundant and the pure metal ion signal needs to be carefully identified.

The method of measuring photoelectron angular distributions has been described earlier.<sup>24,30</sup> Angular distribution measurements were performed on  $\text{Ni}_2^-$  and  $\text{Pd}_2^-$ . In order to extract more information from the angular distribution measurements, additional angular distribution experiments were performed on the coinage metal (Cu, Ag, Au) atoms and dimers.

### III. RESULTS AND ANALYSES

Photoelectron spectra of  $\text{Ni}_2^-$ ,  $\text{Pd}_2^-$ , and  $\text{Pt}_2^-$  are shown in Fig. 1. The photoelectron intensities are plotted as a function of the electron binding energy; no transitions are observed below the low binding energy limits for the three dimers. The considerable variation in signal to noise levels among the three dimers reflects primarily different anion currents and, to a lesser extent, differences in the photodetachment cross sections.

Distinguishable features are observed in each spectrum, as shown in Fig. 1. These features correspond to the ground states or the low-lying excited electronic states of the neutral molecules. There is considerable spectral congestion, caused by vibrational frequencies ( $100\text{--}300\text{ cm}^{-1}$ ) which are comparable to our instrumental resolution ( $8\text{--}10\text{ meV}$ ,  $60\text{--}80\text{ cm}^{-1}$ ), the presence of vibrationally excited anions, and overlap of multiple low-lying neutral electronic excited states. Consequently, definite assignment of every feature is not possible at present. The widths of the sharper vibrational peaks in the three spectra vary from 11 to 20 meV. The small rotational constants of these dimers means that rotational broadening will contribute  $<2\text{ meV}$  to the observed widths; thus the observed broadening must be primarily due to overlapping electronic states, vibrational progressions, and possibly unresolved spin-orbit splittings.

Because a high density of low-lying electronic states can be predicted for the anion dimers as well as for the neutral dimers, it is possible that a number of excited states of  $\text{Ni}_2^-$ ,  $\text{Pd}_2^-$ , and  $\text{Pt}_2^-$  lie very close to the ground state and are appreciably populated given our 300–400 K thermal ion source. However, the widths of the sharp vibrational peaks in the prominent vibronic band systems at lowest energy are primarily instrument limited, and show no evidence of thermal broadening due to noticeable population of more than one electronic state of the anion. Therefore, the strong transitions in the spectra most likely arise from the anion ground electronic states.

#### A. Dinickel

##### 1. Spectrum

The  $\text{Ni}_2^-$  spectrum in Fig. 1 displays several groups of electronic transitions. The largest ion current was only 0.5–1.0 pA, with the result that the spectrum is unusually noisy. The strongest electronic transition, denoted as band X, stands out in the low binding energy region. This band exhibits vibrational progressions that appear to follow a Franck-Condon profile. In addition to band X, there are several features beginning at  $\sim 1.5\text{ eV}$  binding energy and

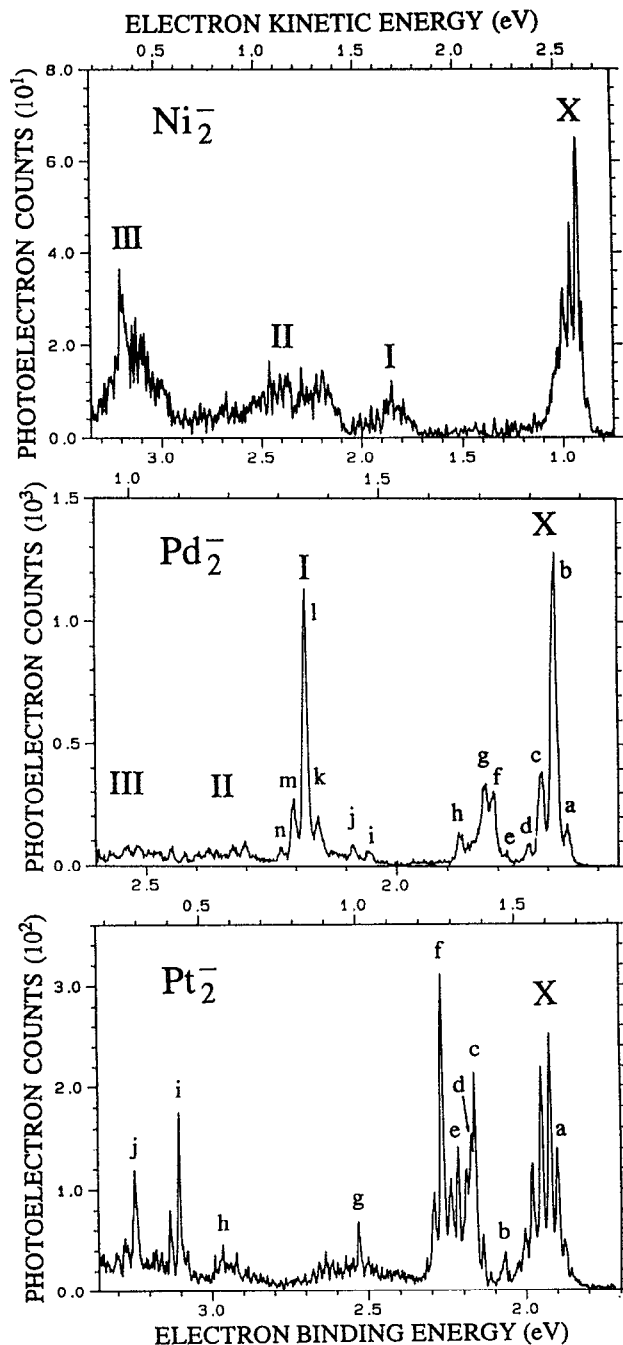


FIG. 1. Photoelectron spectra of  $\text{Ni}_2^-$ ,  $\text{Pd}_2^-$ , and  $\text{Pt}_2^-$  at 351.1 nm (3.531 eV) with 8–10 meV instrumental resolution. The spectra were taken at “magic” angle,  $\theta=54.7^\circ$ , and the photoelectron counts are plotted as a function of the electron binding energy ( $eBE = h\nu - eKE$ ).

extending to the limit of the photon energy. We label these *I* (1.7–2.1 eV), *II* (2.1–2.9 eV), and *III* ( $\geq 2.9\text{ eV}$ ). All of these features are relatively weak and exhibit a nearly continuous spectrum. They are likely composed of many overlapping electronic states. The intensity of *III* at high electron binding energy may be reduced because the instrumental sensitivity degrades rapidly in this region. Since *I*, *II*, and *III* are all diffuse and almost structureless, detailed assignment is not feasible. An assignment has been attempted only for band X.

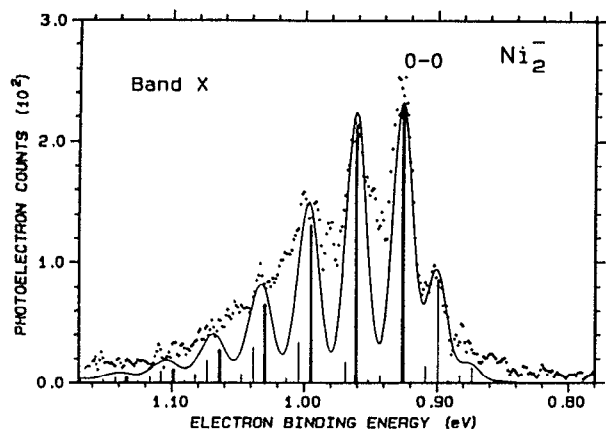


FIG. 2. Expanded portion of band  $X$  of the  $\text{Ni}_2^-$  spectrum. The points represent the experimental data and the solid curve is the Franck–Condon simulation. Individual vibrational transitions are marked with sticks, and the transition origin is marked by a stick with an arrow.

Figure 2 displays an expanded portion of the spectrum containing band  $X$ . The band shows one dominant vibrational progression, and the overall band is  $\sim 150$  meV wide. A Franck–Condon analysis is performed, where the lower anion and upper neutral state potential functions are modeled as simple harmonic oscillators. The procedure of the Franck–Condon analysis has been described earlier.<sup>25,30</sup> Both the anion and neutral molecular constants are fitted simultaneously. The spectral simulation yields the bond length change between the anion and neutral, and an anion temperature of  $250 \pm 50$  K. The determination of the transition origin implies a  $\text{Ni}_2$  electron affinity of  $0.926 \pm 0.010$  eV. The vibrational frequencies are found to be 210 and  $280 \text{ cm}^{-1}$ , respectively for the anion and neutral. The direction of the bond length change cannot be simply determined based on the simulation. However, because of changes in the vibrational frequency and in the dissociation energy discussed in this section, both of which imply a stronger bond in the neutral than in the anion, we assume that the bond length decreases in the transition. Using the neutral bond length of  $2.155 \text{ \AA}$  from high resolution optical spectroscopy,<sup>12</sup> we find the anion bond length to be  $2.257 \text{ \AA}$ . The results of the Franck–Condon analysis are summarized in Table I.

The simulation of band  $X$  shown in Fig. 2 does not account for all of the structure present in the spectrum. Normally, the Franck–Condon simulation gives a very accurate rendition of the spectra of diatomic molecules, such as for the coinage metal dimers,<sup>25</sup>  $\text{Pd}_2$ ,<sup>24</sup> and  $\text{Pt}_2$  in this work. The failure of the simulation to reproduce the data indicates that there is more than one neutral state in this region. These states may be nearly degenerate low-lying electronic states, as predicted by the theoretical calculations. The transitions allowed from the anion ground state to these multiple neutral states produce the congested spectrum.

Using the relationship  $D_0(\text{Ni}_2^-) = D_0(\text{Ni}_2) + \text{EA}(\text{Ni}_2) - \text{EA}(\text{Ni})$ , we can determine the anion dissociation energy. Employing the values  $D_0(\text{Ni}_2) = 2.068 \pm 0.01$  eV from resonant two photon ionization spectroscopy,<sup>11</sup> and  $\text{EA}(\text{Ni}_2)$  and  $\text{EA}(\text{Ni})$  from photoelectron spectroscopy, we obtain  $D_0(\text{Ni}_2^-) = 1.84 \pm 0.03$  eV. The anion dissociation energy is slightly lower than that of the neutral dimer.

## 2. Angular distributions

From angular distribution measurements, the asymmetry parameter  $\beta$  is determined to be  $0.8 \pm 0.3$  for band  $X$ . The asymmetry parameter is measured for the individual peaks, and  $\beta$  is approximately constant over the vibrational progression. Other photoelectron spectroscopy experiments have shown that  $\beta = 2$  for  $s$  orbital detachment from the anions of hydrogen<sup>31</sup> and several alkali metal<sup>32</sup> and transition metal<sup>33</sup> atoms. The angular distribution is expected to be more isotropic for  $d$ -electron detachment than  $s$  electron detachment, and if the transition is not very close to threshold,  $\beta$  for  $d$ -electron detachment is usually negative.<sup>24,33</sup> This difference in anisotropy generally allows us to distinguish detachments from  $s$  and  $d$  orbitals. Angular distribution measurements have also been performed on the coinage metal dimers. Two transitions of  $\text{Cu}_2^-$ , corresponding to  $X^1\Sigma_g^+(s\sigma_g^2) \leftarrow X^2\Sigma_u^+(s\sigma_g^2\sigma_u^{*1})$  and  $a^3\Sigma_u^+(s\sigma_g^1\sigma_u^{*1}) \leftarrow X^2\Sigma_u^+(s\sigma_g^2\sigma_u^{*1})$ , were observed. Removal of one  $s\sigma_u^*$  electron corresponds to the ground to ground state transition with an  $\sim 2.6$  eV electron kinetic

TABLE I. The electronic states and molecular constants of nickel and copper dimers.<sup>a</sup>

Molecule	$\text{Ni}_2^-$	$\text{Ni}_2$	$\text{Cu}_2^-$	$\text{Cu}_2$
Assignment	$X$	$X\Omega=0^b$	$X^2\Sigma_u^+$	$X^1\Sigma_g^+$
Config.	$3d^{18}(\delta\delta)(4s\sigma_g)^2(4s\sigma_u)$	$3d^{18}(\delta\delta)(4s\sigma_g)^2$	$3d^{20}(4s\sigma_g)^2(4s\sigma_u)$	$3d^{20}(4s\sigma_g)^2$
$\omega_e$ ( $\text{cm}^{-1}$ )	$210 \pm 25$	$280 \pm 20$	$196 \pm 15$	266.43
$r_e$ ( $\text{\AA}$ ) <sup>b</sup>	$2.257 \pm 0.017$	$2.155 \pm 0.007^b$	$2.343 \pm 0.007$	2.2197
$D_0$ (eV)	$1.84 \pm 0.03$	$2.068 \pm 0.01^b$	$1.62 \pm 0.09$	$2.02 \pm 0.08$
Intrinsic bond strength (eV) <sup>c</sup>	$1.86 \pm 0.03$	$2.119 \pm 0.01$	$1.62 \pm 0.09$	$2.02 \pm 0.08$
$k$ ( $\text{mdyn/\AA}$ )	0.76	1.36	0.73	1.34
EA (eV)		$0.926 \pm 0.010$		$0.836 \pm 0.06$

<sup>a</sup>Data for  $\text{Cu}_2$  and  $\text{Cu}_2^-$  are from Ref. 25.

<sup>b</sup>References 11 and 12.

<sup>c</sup>The intrinsic bond strength is the sum of  $D_0$  and the promotion energy of the atomic asymptote.

energy, and  $\beta$  is measured to be  $0.8 \pm 0.3$ ; removal of an  $s\sigma_g$  electron corresponds to an excited state transition, and  $\beta$  for this band at around 0.8 eV electron kinetic energy is  $1.5 \pm 0.3$ . The experiments show that detachment from the  $4s\sigma_g(\text{Cu}_2)$  orbitals is almost completely  $s$ -like ( $\cos^2 \theta$  distribution), while the  $4s\sigma_u^*$  electron detachments are not as strongly peaked along the electric vector. One explanation is based on the orbital symmetry. In contrast to the highly symmetric  $\sigma_g$  orbital, the  $\sigma_u^*$  orbital is antisymmetric ( $p$ -like) with respect to the reflection through the central plane perpendicular to the molecular axis.

Band  $X$  of  $\text{Ni}_2^-$  has the same  $\beta$  value of  $0.8 \pm 0.3$  and similar electron kinetic energy to the ground state transition of  $\text{Cu}_2^-$ . This similarity suggests that the band  $X$  transition in the  $\text{Ni}_2^-$  spectrum also arises from  $s\sigma_u^*$  electron detachment, as in the  $X^1\Sigma_g^+(4s\sigma_g^2) \leftarrow X^2\Sigma_u^+(4s\sigma_g\sigma_u^*)$  transition of  $\text{Cu}_2^-$ .

### 3. Analysis

The  $\text{Ni}_2^-$  spectrum is much more complex than that of the corresponding coinage metal dimer,  $\text{Cu}_2^-$ .<sup>25</sup> Because of an open  $3d$  subshell in the  $\text{Ni}_2$  molecule, the density of the low-lying electronic states increases dramatically. The Ni atom has a  $^3F_4(3d^84s^2)$  ground state and the first excited state,  $^3D_3(3d^94s^1)$ , lies only  $204.8 \text{ cm}^{-1}$  above the ground state.<sup>29</sup> Although the open  $d$  shell creates the possibility for  $d$  electrons to participate in bonding, *ab initio* calculations predict that the chemical bonding in  $\text{Ni}_2$  originates primarily from the interactions of the  $4s$  orbitals, and the  $3d^9$  cores only weakly interact.<sup>5,7</sup> The ground state of  $\text{Ni}_2$  is expected to arise from a  $3d^{18}4s^2(\sigma_g^2)$  configuration, which has a ( $\sigma$ ) bond order of 1 and can be formed from the coupling of two Ni atoms in the  $^3D$  state. A simplified notation is employed, in which all the  $d$  electrons from the two constituent atoms are summed together and only the  $s\sigma$  molecular orbitals are given along with the  $s$  electronic configurations. The coupling of two  $^3D$  atoms gives at least 30 chemically bound molecular states. These states can be considered as having two  $3d$  holes, which result in the six possible  $3d$  shell configurations  $\sigma\sigma, \sigma\pi, \sigma\delta, \pi\pi, \pi\delta$ , and  $\delta\delta$ . The most accurate *ab initio* calculations find<sup>5,7</sup> that the six states arising from the  $\delta\delta$  configuration are stabilized relative to states of other configurations and are nearly degenerate.

There have been no *ab initio* calculations or previous experiments on  $\text{Ni}_2^-$ . Photoelectron spectroscopy has shown that the ground state of  $\text{Ni}^-$  is  $^2D_{5/2}(3d^94s^2)$ , and the lowest excited state is  $^2D_{3/2}$  lying  $1470 \text{ cm}^{-1}$  above the ground state.<sup>28</sup> Another atomic excited state of the anion which may correlate with the dimer ground state is  $^2S(3d^{10}4s^1)$ , but no experimental data regarding this state have been reported. The interaction of the ground states of the neutral atom ( $^3F$ ) and the anion ( $^2D$ ) forms a  $3d^{17}4s^4(\sigma_g^2\sigma_u^{*2})$  molecule with a bond order of 0. The interaction of the  $^3D$  atom with the  $^2D$  anion can form a  $3d^{18}(4s\sigma_g)^2(4s\sigma_u^*)$  molecule with a bond order of 1/2; a promotion energy of only  $204 \text{ cm}^{-1}$  is paid for the bonding. In addition, the interaction of  $\text{Ni } ^3D$  and  $\text{Ni}^- ^2S$  can

TABLE II. Configurations of low-lying electronic states of  $\text{Ni}_2^-$ ,  $\text{Ni}_2$ ,  $\text{Pt}_2^-$ , and  $\text{Pt}_2$ , with their dissociation asymptotes and corresponding atomic promotion energies.

Config. <sup>a</sup>	Asymptotic atomic state	Promotion energy <sup>b</sup> $\text{cm}^{-1}$	$\sigma$ bond order
<b><math>\text{Ni}_2</math></b>			
$3d^{16}4s^4(\sigma_g^2\sigma_u^2)$	$^3F(3d^84s^2) + ^3F(3d^84s^2)$	0	0
$3d^{17}4s^3(\sigma_g^2\sigma_u^1)$	$^3F(3d^84s^2) + ^3D(3d^94s^1)$	204	1/2
$3d^{18}4s^2(\sigma_g^2)$	$^3D(3d^94s^1) + ^3D(3d^94s^1)^c$	408	1
<b><math>\text{Ni}_2^-</math></b>			
$3d^{17}4s^4(\sigma_g^2\sigma_u^2)$	$^3F(3d^84s^2) + ^2D(3d^94s^2)$	0	0
$3d^{18}4s^3(\sigma_g^2\sigma_u^1)$	$^3D(3d^94s^1) + ^2D(3d^94s^2)^c$	204	1/2
<b><math>\text{Pt}_2</math></b>			
$5d^{18}6s^2(\sigma_g^2)$	$^3D(5d^96s^1) + ^3D(5d^96s^1)^c$	0	1
<b><math>\text{Pt}_2^-</math></b>			
$5d^{18}6s^3(\sigma_g^2\sigma_u^1)$	$^3D(5d^96s^2) + ^2D(5d^96s^2)^c$	0	1/2

<sup>a</sup>Only the  $s\sigma$  bond is considered and expressed in the table.

<sup>b</sup>The values are from Ref. 29.

<sup>c</sup>The ground state assigned in this work.

form a strongly bound molecule,  $3d^{19}4s^2(\sigma_g^2)$ , with a full  $\sigma$  bond; but one pays a promotion energy of  $204 \text{ cm}^{-1}$  plus an unknown amount.

When assigning the possible transitions, it is important to note two major propensity rules of electron photodetachment.<sup>34,35</sup> (1) In general, single electron processes (i.e., detachment with no additional electron reorganization) are expected to give rise to the strongest photoelectron transitions. (2) Processes involving  $s$  electron detachment are expected to have larger cross sections than those involving  $d$  electron detachment (within 1–2 eV above threshold). In addition, the Franck–Condon analysis shows a lower vibrational frequency and a smaller bond strength for the anion, suggesting that the photoelectron may be detached from an antibonding orbital. Based on this information, we assign band  $X$  to a  $4s\sigma_u^*$  electron detachment. This assignment is also consistent with the angular distribution measurements.

The  $3d^{19}(4s\sigma_g)^2$  configuration can be ruled out as being the anion ground state, as  $s\sigma_u^*$  electron detachment is observed. The  $3d^{17}(4s\sigma_g)^2(4s\sigma_u^*)^2$  configuration is also unlikely to be the ground state configuration. In spite of correlating to the lowest dissociation asymptote, this state in first order is only weakly bound as a van der Waals molecule. Moreover, the appearance of the spectrum is unlike an  $s\sigma_u^*$  electron detachment from the  $3d^{17}(4s\sigma_g)^2(4s\sigma_u^*)^2$  configuration. The  $4s\sigma_u^*$  detachment would lead to two final states, depending on the high- or low-spin coupling between the remaining  $4s\sigma_u^*$  electron and the  $3d^{17}$  “core.” Normally, transitions from the anion to these two states display two intense bands with similar vibrational progressions, as in the spectra of  $\text{Pd}_2$  (Ref. 24) or  $\text{Fe}_2$ .<sup>36</sup> Therefore, we assign the remaining choice,  $3d^{18}(4s\sigma_g)^2(4s\sigma_u^*)$ , to the  $\text{Ni}_2^-$  ground state. The most likely ground state configurations of  $\text{Ni}_2$  and  $\text{Ni}_2^-$ , along with their lowest dissociation asymptotes, are listed in Table II.

We assign band *X* as originating from the anion ground state. Since we do not know the *3d* shell configuration for the anion, we cannot immediately determine whether the *X* band terminates in one of the lowest electronic states with a  $\delta\delta$  configuration or in higher excited states corresponding to other configurations. Although the propensity for single electron processes will favor transitions to states with the same *3d* shell configuration as in the anion, the predicted<sup>7,37</sup> spin-orbit mixing between states of  $\delta\delta$  and  $\delta\pi$  configuration could give strength to other transitions as well. Therefore, a definite assignment of the *d* hole configuration of the  $\text{Ni}_2^-$  ground state from this experiment is difficult. However, we can make a tentative assignment, neglecting the spin-orbit mixing. *Ab initio* calculations suggest that the electronically excited states of all *3d* shell configurations other than  $\delta\delta$  lie at least 0.2 eV above the ground state.<sup>5,7,37</sup> If we were to assume that the *3d* shell configuration of the anion ground state differs from that of the neutral and assign band *X* to a  $\text{Ni}_2$  excited state, then the adiabatic electron affinity (EA) would be at least 0.2 eV lower than the measured value of 0.926 eV. This value is much smaller than the  $\text{Fe}_2$  and  $\text{Co}_2$  electron affinities ( $0.902 \pm 0.008$  and  $1.110 \pm 0.008$  eV),<sup>36</sup> and even smaller than that of  $\text{Cu}_2$  ( $0.836 \pm 0.006$  eV). This is unlikely, because  $\text{Cu}_2$   $3d^{20}(4s\sigma_g)^2$  has the most stable configuration of the first row transition metal dimers, and should have a relatively small electron affinity. Since  $\text{Fe}_2$ ,  $\text{Co}_2$ , and  $\text{Ni}_2$  have open *3d* shells, the shielding effect of the *3d* shell for valence *4s* electrons is smaller than for  $\text{Cu}_2$ . The detaching  $4s\sigma_g^*$  electron feels a stronger core potential, resulting in a larger EA for  $\text{Ni}_2$ , as well as for  $\text{Fe}_2$  and  $\text{Co}_2$ . The larger EAs for  $\text{Fe}_2$  and  $\text{Co}_2$  are experimentally verified<sup>36</sup> and, given the present result of  $\text{EA}(\text{Ni}_2) = 0.926$  eV, it is reasonable to assign band *X* to the  $\delta\delta$  neutral ground state or nearby low-lying state(s) with the same  $\delta\delta$  configuration.

It still cannot be inferred from the vibrational data alone that the dominant vibrational progression observed in the photoelectron spectrum arises from the  $\text{Ni}_2$  ground state. Since the multiple low-lying states lie close to one another and originate from the same molecular orbital configuration, their molecular constants are expected to be similar. The results in the present work therefore should properly be considered to be approximate molecular constants (including EA) of the  $\text{Ni}_2$  ground state. We further assert that the anion has the same *3d* shell  $\delta\delta$  configuration as the neutral ground state. The  $\text{Ni}_2^-$  ground state is thus well characterized by the present experimental results.

## B. Diplatinum

### 1. Spectrum

The  $\text{Pt}_2^-$  spectrum in Fig. 1 shows rich structure containing resolved vibrational progressions along with diffuse electronic bands. At the lowest electron binding energy, the spectrum shows an electronic band with a Franck-Condon vibrational progression. The band is labeled *X*, implying that it corresponds to the neutral ground state. In the next region (2.05–2.35 eV), at least ten single vibra-

TABLE III. Measurements of several transitions of  $\text{Pt}_2^-$ .

Band	Vibrational origin <sup>a</sup>	Binding energy (eV)	$ r'_e - r''_e $ (Å)	$\omega$ ( $\text{cm}^{-1}$ )
<i>X</i> (1.8–2.1 eV)	a	$1.899 \pm 0.008$	$0.074 \pm 0.008$	$215 \pm 15$
<i>I</i>	b <sup>b</sup>	$2.07 \pm 0.01$		
<i>II</i>	c	$2.16 \pm 0.01$	$\sim 0.04$	$205 \pm 30$
<i>III</i>	d	$2.17 \pm 0.02$	$\sim 0.03$	$200 \pm 40$
<i>IV</i>	e	$2.22 \pm 0.01$	$0.05 \pm 0.02$	$190 \pm 25$
<i>V</i>	f	$2.26 \pm 0.01$	$0.03 \pm 0.02$	$205 \pm 25$
	g <sup>b</sup>	$2.53 \pm 0.01$		
	h <sup>b</sup>	$2.97 \pm 0.01$		
<i>VI</i>	i	$3.104 \pm 0.010$	$0.040 \pm 0.015$	$215 \pm 20$
<i>VII</i>	j	$3.243 \pm 0.010$	$0.040 \pm 0.020$	$215 \pm 25$

<sup>a</sup>Peaks are labeled in Fig. 1.

<sup>b</sup>Peak with a relatively strong intensity in a broad feature; it may not necessarily correspond to the vibrational origin.

tional peaks are discernible. Based on the uneven intensity distribution and the peak spacings, several overlapping electronic transitions must be responsible for the features. We have identified no fewer than five electronic states. The intensities of these bands are comparable with band *X*. In the 2.37–3.05 eV region, the spectrum shows weak and diffuse features along with a few sharp vibrational peaks. These features most likely arise from many weak electronic transitions, and possibly extend into the neighboring energy regions. Only the positions of two of the strongest sharp peaks are reported. In the highest energy region (3.05–3.34 eV), two distinct electronic bands are observed. Both bands show resolved vibrational structure, and these progressions are shorter than that of band *X*. The positions of the proposed transition origins are listed in Table III.

A Franck-Condon analysis has been carried out on band *X*, with the results displayed in Fig. 3. Since the peak corresponding to the vibrational transition origin is not at all obvious, several possible assignments were attempted; only one choice yielded both a satisfactory optimized fit and a reasonable anion vibrational temperature ( $250 \pm 50$  K). The results are summarized in Table IV, and give

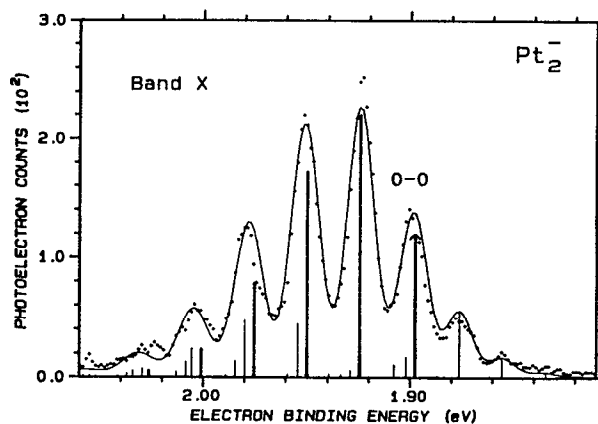


FIG. 3. Expanded portion of band *X* of the  $\text{Pt}_2^-$  spectrum. The points represent the experimental data and the solid curve is the optimized Franck-Condon simulation. Individual vibrational transitions are marked with sticks, and the transition origin is marked by a stick with an arrow.

TABLE IV. The electronic ground states and molecular constants of platinum and gold dimers.<sup>a</sup>

Molecule	Pt <sub>2</sub> <sup>-</sup>	Pt <sub>2</sub>	Au <sub>2</sub> <sup>-</sup>	Au <sub>2</sub>
Assignment	<i>X</i>	<i>X</i>	<i>X</i> <sup>2Σ<sub>g</sub><sup>+</sup></sup>	<i>X</i> <sup>1Σ<sub>g</sub><sup>+</sup></sup> (0 <sub>g</sub> <sup>+</sup> )
Config.	5 <i>d</i> <sup>18</sup> (6 <i>s</i> σ <sub>g</sub> ) <sup>2</sup> (6 <i>s</i> σ <sub>u</sub> )	5 <i>d</i> <sup>18</sup> (6 <i>s</i> σ <sub>g</sub> ) <sup>2</sup>	5 <i>d</i> <sup>20</sup> (6 <i>s</i> σ <sub>g</sub> ) <sup>2</sup> (6 <i>s</i> σ <sub>u</sub> )	5 <i>d</i> <sup>20</sup> (6 <i>s</i> σ <sub>g</sub> ) <sup>2</sup>
ω <sub>e</sub> (cm <sup>-1</sup> )	178±20	215±15	149±10	190.9
r <sub>e</sub> (Å)	(r <sub>e</sub> <sup>+</sup> + 0.074) ± 0.008	r <sub>e</sub> <sup>b</sup>	2.582±0.007	2.4719
D <sub>0</sub> (eV) <sup>c</sup>	2.91±0.03	3.14±0.02 <sup>d</sup>	1.92±0.15	2.29±0.02
Intrinsic bond strength (eV) <sup>c</sup>	2.91±0.03	3.14±0.02 <sup>d</sup>	1.92±0.15	2.29±0.02
k (mdyn/Å)	1.82	2.66	1.29	2.12
EA (eV)		1.898±0.008		1.938±0.006

<sup>a</sup>Data for Au<sub>2</sub> and Au<sub>2</sub><sup>-</sup> are from Ref. 25.

<sup>b</sup>A recent experiment suggests that the average bond length of Pt<sub>2</sub> on a graphite substrate is 2.45 Å. See, U. Muller, K. Sattle, J. Xhie, N. Venkateswaran, and G. Raina, *J. Vac. Sci. Technol. B* **9**, 829 (1991).

<sup>c</sup>Since no promotion energy is required for any of the ground states, D<sub>0</sub> and the intrinsic bond strength are the same for all species.

<sup>d</sup>See Ref. 17.

EA(Pt<sub>2</sub>) = 1.898 ± 0.008 eV, and vibrational frequencies 215 ± 15 and 178 ± 20 cm<sup>-1</sup> for the neutral and anion, respectively. Using D<sub>0</sub>(Pt<sub>2</sub><sup>-</sup>) = D<sub>0</sub>(Pt<sub>2</sub>) + EA(Pt<sub>2</sub>) - EA(Pt), D<sub>0</sub>(Pt<sub>2</sub>) = 3.14 ± 0.02 eV from optical spectroscopy,<sup>17</sup> and EA(Pt<sub>2</sub>) and EA(Pt) (Ref. 28) from photoelectron spectroscopy, we obtain D<sub>0</sub>(Pt<sub>2</sub><sup>-</sup>) = 2.91 ± 0.03 eV. Like dinickel, the anion dissociation energy is slightly lower than that of the neutral dimer. The Franck-Condon simulation yields a bond length change of 0.074 ± 0.008 Å, and, based on the observed change in vibrational frequency and dissociation energy, we assume that the anion bond length is larger than that of the neutral.

Crude analyses of the electronic transitions (origins are assigned to *b*-*f*, *i*, and *j*) are presented in Table III. All of these bands have narrower vibrational progressions than band *X*, suggesting the transitions are more vertical. Comparison of the Ni<sub>2</sub><sup>-</sup> and Pt<sub>2</sub><sup>-</sup> spectra shows a marked difference; multiple strong transitions at energies 1200–3600 cm<sup>-1</sup> above the ground state are observed in the Pt<sub>2</sub><sup>-</sup> spectrum, but no strong transitions are present in the corresponding energy range for Ni<sub>2</sub><sup>-</sup>. Since the spin-orbit interaction is expected to be significant for heavy diatomic system like Pt<sub>2</sub>,<sup>14</sup> the neutral excited states of Pt<sub>2</sub> in this region may arise from spin-orbit splittings. No specific assignments have been made for these states.

## 2. Analysis

Pt has a <sup>3</sup>D<sub>3</sub>(5*d*<sup>9</sup>6*s*<sup>1</sup>) ground state. The combination of two <sup>3</sup>D Pt atoms forms a 5*d*<sup>18</sup>6*s*<sup>2</sup>(σ<sub>g</sub><sup>2</sup>) molecule. The other low-lying excited states of Pt are <sup>3</sup>F<sub>4</sub>(5*d*<sup>8</sup>6*s*<sup>2</sup>) and <sup>1</sup>S(5*d*<sup>10</sup>).<sup>29</sup> The Pt<sub>2</sub> electronic states arising from combinations of the <sup>3</sup>D atom with the <sup>3</sup>F or <sup>1</sup>S atom (or two <sup>3</sup>F or <sup>1</sup>S atoms) are not likely to be deeply bound in comparison to the states arising from two <sup>3</sup>D atoms because, like Ni<sub>2</sub>, Pt<sub>2</sub> is described<sup>13</sup> as primarily bonded through a (6*s*σ<sub>g</sub>)<sup>2</sup> single bond. The 5*d* shell contains two holes which can form six configurations by filling *d*σ, *d*π, and *d*δ orbitals, and the lowest state should have a δδ configuration. Balasubramanian has investigated Pt<sub>2</sub>,<sup>14</sup> and introduced the spin-orbit interaction through relativistic configuration interactions. He predicted the ground states to be

(δ<sub>u</sub>)<sup>2</sup> <sup>3</sup>Σ<sub>g</sub><sup>-</sup>(0<sub>g</sub><sup>+</sup>), and the lowest excited state, δ<sub>u</sub>δ<sub>g</sub><sup>3</sup>Γ<sub>u</sub>(5<sub>u</sub>), to be only 614 cm<sup>-1</sup> above the ground state.

The ground state of Pt<sub>2</sub><sup>-</sup> has never been studied experimentally or theoretically. The analysis can be simplified by analogy with Ni<sub>2</sub><sup>-</sup>. The Pt<sub>2</sub><sup>-</sup> ground state is <sup>2</sup>D<sub>5/2</sub>(5*d*<sup>9</sup>6*s*<sup>2</sup>). Other Pt<sub>2</sub><sup>-</sup> excited states possibly important for bonding, such as <sup>2</sup>S(5*d*<sup>10</sup>6*s*<sup>1</sup>), may lie too high to be correlated with the Pt<sub>2</sub><sup>-</sup> ground state. The interaction of the <sup>3</sup>D ground state atom with the <sup>2</sup>D anion forms a 5*d*<sup>18</sup>6*s*<sup>3</sup>(σ<sub>g</sub><sup>2</sup>σ<sub>u</sub><sup>\*1</sup>) molecule. The interaction of the <sup>3</sup>F atom with the <sup>2</sup>D anion forms a 5*d*<sup>17</sup>6*s*<sup>4</sup>(σ<sub>g</sub><sup>2</sup>σ<sub>u</sub><sup>\*2</sup>) molecule, with a nominal bond order of 0 and a promotion energy of 823 cm<sup>-1</sup>. Hence, we tentatively assign the Pt<sub>2</sub><sup>-</sup> ground state as 5*d*<sup>18</sup>6*s*<sup>3</sup>(σ<sub>g</sub><sup>2</sup>σ<sub>u</sub><sup>\*1</sup>). The most likely ground state configurations, along with their lowest dissociation asymptotes, are listed in Table II.

The Pt<sub>2</sub> vibrational frequency and dissociation energy are greater than those of Pt<sub>2</sub><sup>-</sup>, implying that the electron is detached from an antibonding orbital. In addition, all the bands in the Pt<sub>2</sub><sup>-</sup> spectrum are found to be severely congested except for band *X* which is relatively isolated. A natural conclusion is that band *X* arises from a ground to ground state transition with 6*s*σ<sub>u</sub><sup>\*</sup> detachment. If the 5*d* hole configuration of the anion ground state is the same as for the neutral, band *X* can be simply assigned to the neutral ground state. However, if the anion and the neutral 5*d* configurations are not the same, then there are two possibilities. First, the transition can still be assigned to the neutral ground state because it is likely that the ground to ground state transition is detectable in a complex heavy system even where *d* shell configuration changes in going from the anion to the neutral, due to strong configuration mixing. The second possibility is that band *X* corresponds to a neutral low-lying excited state with the same 5*d* configuration as that of the anion. Unlike Ni<sub>2</sub>, some excited states of Pt<sub>2</sub> which are not δδ could lie very close to the ground state because of profound spin-orbit interaction and electron correlation effects.<sup>14</sup> Therefore, only likely assignments are provided, and the molecular constants for the assumed ground states are included in Table IV. For

TABLE V. The electronic states and molecular constants of palladium and silver dimers.<sup>a</sup>

Molecule assignment config.	Pd <sub>2</sub> <sup>-</sup> $X^2\Sigma_u^+$ ( $4d^{19}\sigma_u$ )( $5s\sigma_g$ ) <sup>2</sup>	Pd <sub>2</sub> $X^3\Sigma_u^+$ ( $4d^{19}\sigma_u$ )( $5s\sigma_g$ ) <sup>1</sup>	Pd <sub>2</sub> $^1\Sigma_u^+$ ( $4d^{19}\sigma_u$ )( $5s\sigma_g$ ) <sup>1</sup>	Ag <sub>2</sub> <sup>-</sup> $X^2\Sigma_u^+$ $4d^{20}(5s\sigma_g)^2(5s\sigma_u)$	Ag <sub>2</sub> $X^1\Sigma_u^+$ $4d^{20}(5s\sigma_g)^2$
$\omega_e$ (cm <sup>-1</sup> )	206 ± 15	210 ± 10	200 ± 15	145 ± 10	192.4
$r_e$ (Å)	( $r_e^a - 0.037$ )	$r_e^{b,c}$	( $r_e^a - 0.007$ )	( $r_e^a + 0.124$ )	$r_e^c$
$D_0$ (eV)	2.15 ± 0.17	1.03 ± 0.16 <sup>d</sup>		1.92 ± 0.15	2.29 ± 0.02
Intrinsic bond strength (eV) <sup>e</sup>	2.29 ± 0.17	1.84 ± 0.16		1.92 ± 0.15	2.29 ± 0.02
$k$ (mdyn/Å)	1.32	1.37	1.24	0.66	1.17
EA (eV)		1.685 ± 0.008			1.938 ± 0.007

<sup>a</sup>Data for Ag<sub>2</sub> and Ag<sub>2</sub><sup>-</sup> are from Ref. 25.

<sup>b</sup>The absolute value of the Pd<sub>2</sub> bond length cannot be obtained from this work. A recent calculation reported in Ref. 1 suggests  $r_e^a \approx 2.48$  Å for Pd<sub>2</sub>.

<sup>c</sup>The Ag<sub>2</sub> bond length is also not well known. A somewhat uncertain assignment [V. I. Srdanov and D. S. Pestic, *J. Mol. Spectrosc.* **90**, 27 (1981)] gives  $r_e^c = 2.48$  Å, the same as for Pd<sub>2</sub>.

<sup>d</sup>Shim and Gingerich, Ref. 18.

<sup>e</sup>The intrinsic bond strength is the sum of  $D_0$  and the promotion energy of the atomic asymptote.

the neutral excited states, no detailed assignments have been attempted.

### C. Dipalladium

The Pd<sub>2</sub><sup>-</sup> spectrum in Fig. 1 shows 14 prominent peaks labeled by letters a to n. Two strong electronic transitions stand out in the spectrum, the vibrational peaks a, b, c, and d form one electronic band, and peaks l, m, and n form another one. The two bands have nearly identical Franck-Condon vibrational profiles and transition intensities. The band with lowest electron binding energy is labeled *X* and assigned to the neutral ground state, and the other band is labeled *I* for reference. The bands show only three to four sequential vibrational transition peaks, suggesting that the electronic transitions are nearly vertical with small bond length changes. The linewidths of the single peaks (b and l for example) are close to the instrumental resolution, implying that they contain mainly one vibrational transition.

The appearance of the Pd<sub>2</sub><sup>-</sup> spectrum is quite different from the Ni<sub>2</sub><sup>-</sup> and Pt<sub>2</sub><sup>-</sup> spectra. The band widths of the two strongest bands (*X* and *I*) are much narrower than those of band *X* in the Ni<sub>2</sub><sup>-</sup> and Pt<sub>2</sub><sup>-</sup> spectra. The Pd<sub>2</sub><sup>-</sup> spectrum shows fewer transitions; only weak and broad features are observed in the 2.2–2.6 eV region and no strong transitions are observed above 2.6 eV. The spectrum can be better understood in terms of the analysis of the possible electron configurations of Pd<sub>2</sub> and Pd<sub>2</sub><sup>-</sup>. Pd has a unique closed-shell electronic ground state,  $^1S_0(4d^{10}5s^0)$ . In a first order approximation, the combination of Pd  $^1S_0$  atoms only forms a weakly bound van der Waals molecule. To increase the bonding, at least one *4d* electron must be excited to a *5s* orbital on one or both atoms. The interaction of an excited Pd  $^3D(4d^95s^1)$  with a  $^1S_0$  atom forms an *σ* bond with a bond order of 1/2, but the promotion energy<sup>29</sup> required is 6564 cm<sup>-1</sup>. Likewise, two  $^3D$  atoms can generate a bound state with a bond order of 1, but twice the promotion energy is required. For the anion, Pd<sup>-</sup> has a ground state  $^2S_{1/2}(4d^{10}5s^1)$ ,<sup>28</sup> and an excited state,  $^2D_{5/2}(4d^95s^2)$  lying only 1113 cm<sup>-1</sup> above the ground state. The interaction of

Pd<sup>-</sup> ( $^2S_{1/2}$ ) and the neutral atom ( $^1S_0$ ) forms a molecular anion  $4d^{20}(5s\sigma_g)^1$  with a bond order of 1/2. The interaction of the Pd  $^1S_0$  atom with the excited state anionic atom  $^2D_{5/2}$  can form a  $4d^{19}(5s\sigma_g)^2$  molecular anion with a bond order of 1; in this case, one pays a considerably smaller promotion energy than for the neutral. The interaction of the  $^1S_{1/2}$  anion with the  $^3D$  atom can also form a bonding molecule, but must pay the same 6564 cm<sup>-1</sup> promotion energy as in the neutral case. Finally, combining the Pd<sup>-</sup>  $^2D_{5/2}$  and the Pd  $^3D$  atom forms a  $4d^{18}(5s\sigma_g)^2(5s\sigma_u)^1$  molecule with a bond order of 1/2. Because of this complicated situation, the determination of the electronic structures of Pd<sub>2</sub> and Pd<sub>2</sub><sup>-</sup> becomes particularly interesting.

The two strong electronic bands (*X* and *I*) have been analyzed in great detail in a previous paper.<sup>24</sup> The anion electronic ground state is assigned to  $X^2\Sigma_u^+[(4d^{19}\sigma_u)(5s\sigma_g)^2]$ , and the two neutral states corresponding to bands *X* and *I* are assigned to  $X^3\Sigma_u^+[(4d^{19}\sigma_u)(5s\sigma_g)^1]$  and  $^1\Sigma_u^+[(4d^{19}\sigma_u)(5s\sigma_g)^1]$ . The main results are summarized in Table V. For the peaks and features lying between the *X* and *I* bands and above band *I*, some possible assignments have also been suggested.<sup>24</sup>

### IV. DISCUSSION

For the nickel and platinum dimers, the dissociation energy of the anion is ~10%–15% less than that of the neutral; for palladium, the dissociation energy of the anion is twice that of the neutral. This reflects the dramatic difference in the ground state configurations between palladium dimer and the other dimers.<sup>2,25</sup> For nickel and platinum dimers, the electronic configurations of the anion and the neutral are  $nd^{18}[(n+1)(s\sigma_g)^2(s\sigma_u^*)]$  and  $nd^{18}[(n+1)(s\sigma_g)^2]$ , respectively. The dissociation energies of the neutral dimers are larger than those of the anion dimers,<sup>25</sup> as is predicted from the simple molecular orbital arguments. The MO configurations of the palladium anion and neutral dimers assigned are  $4d^{19}(5s\sigma_g)^2$  and  $4d^{19}(5s\sigma_g)^1$ , respectively. This assignment reflects the bond strength of the anion dimer being larger than that of the neutral dimer.

The reason for the unusually small dissociation energy of Pd<sub>2</sub> compared to the other nickel group metal dimers is the extra promotion energy required for *sσ* bonding. Therefore, the special character of the palladium dimer can be attributed to the stable (4*d*<sup>10</sup>) ground state of the Pd atom.

The nickel group dimer spectra are much more complicated than the coinage metal dimer spectra. A large number of neutral low-lying electronic excited states are observed, especially in the Ni<sub>2</sub><sup>-</sup> and Pt<sub>2</sub><sup>-</sup> spectra. Although restricted by the photodetachment propensities, the spectra still reflect the very large density of low-lying electronic states in the nickel group dimers. From the general appearances of the three spectra, we find that in our photon energy range, the density of the electronic states increases in the order Pd<sub>2</sub> < Pt<sub>2</sub> < Ni<sub>2</sub>. Pd<sub>2</sub> exhibits a relatively low density of electronic states because Pd has a very stable 4*d*<sup>10</sup> ground state. The density of electronic states stays low until the states resulting from the combination of two <sup>3</sup>D atoms are reached. After that the density of Pd<sub>2</sub> states increases rapidly. Ni<sub>2</sub> displays the highest density of electronic states. Except for the region of band X, the spectrum has diffuse and almost continuous band features. Pt<sub>2</sub> also has a high density of states, but most of the low-lying states are still distinguishable in the spectrum. The decreased density of the electronic states in Pt<sub>2</sub> compared to Ni<sub>2</sub> is due in part to greater *d-d* orbital splittings as the *d* orbital participation in bonding increases. Stronger relativistic interactions, such as spin-orbit splitting in Pt<sub>2</sub>, also contribute to a decreased electronic state density. Recently, Morse has calculated the number of distinct electronic states that arise from the combination of the separated atoms.<sup>2</sup> According to his calculation, the number of states within 2500 cm<sup>-1</sup> of the ground state for Ni<sub>2</sub> is above 500; the corresponding number of states for Pt<sub>2</sub> is less than for Ni<sub>2</sub>, but still exceeds 250.

Morse and co-workers<sup>2</sup> have conducted a thorough comparison of the neutral dimers of the nickel and coinage metal groups. It is interesting to compare bonding in these two groups again, in light of the new negative ion data. For the coinage metal dimers, the contribution of the *d*-electrons to bonding is negligible because of the closed *d* shell configurations; the chemical bonding is ascribed entirely to the *sσ* orbital contribution. The comparison helps in assigning the spectra of the nickel group dimers and is expected to provide insight into the *d* orbital contribution to the chemical bonding. The molecular constants for the coinage metal dimers are listed along with their corresponding nickel group dimers in Tables I, IV, and V. To reflect properly the magnitude of *d*-orbital participation in bonding, we choose to compare intrinsic bond strengths (*D*<sub>0</sub>+promotion energy of atomic asymptote), rather than the actual dissociation energies. In fact, the difference between the two quantities is negligible for all species except Pd<sub>2</sub>.

Comparing the nickel and copper molecular constants in Table I, we find that the anion and neutral bond strengths and the bond length changes between the anion and neutral are nearly the same. The vibrational frequencies are slightly different; however, the force constants (*k*)

determined using the relation  $\omega_e^2 = 4\pi^2 k/\mu$  ( $\mu$  is the reduced mass) are nearly the same. The similarity of the bond strengths and force constants suggests that the 3*d* contribution to the bonding in both Ni<sub>2</sub><sup>-</sup> and Ni<sub>2</sub> is minor, and that the (4*sσ<sub>g</sub>*)<sup>2</sup> contribution dominates the bonding. The analogy to Cu<sub>2</sub><sup>-</sup> strongly supports the assignment of the Ni<sub>2</sub><sup>-</sup> anion ground state as 3*d*<sup>18</sup>( $\delta_u^2$ )4*s*<sup>3</sup>( $\sigma_g^2\sigma_u^*$ ).

Comparison of the platinum and gold dimers shows a substantial difference. From Table IV, we see that the Pt<sub>2</sub> and Pt<sub>2</sub><sup>-</sup> bond strengths are substantially greater than those of Au<sub>2</sub> and Au<sub>2</sub><sup>-</sup>, respectively. Also, the bond length change from anion to neutral upon the 6*sσ<sub>u</sub>*<sup>\*</sup> detachment is smaller for Pt<sub>2</sub><sup>-</sup> (0.07 Å) than for Au<sub>2</sub><sup>-</sup> (0.11 Å). In contrast to nickel dimer, the force constants of Pt<sub>2</sub> and Pt<sub>2</sub><sup>-</sup> are also considerably larger than those of Au<sub>2</sub> and Au<sub>2</sub><sup>-</sup>. This difference is explained qualitatively by the participation of 5*d* electrons in the bonding of Pt<sub>2</sub><sup>-</sup> and Pt<sub>2</sub>. The existence of *d* bonds in Pt<sub>2</sub><sup>-</sup> and Pt<sub>2</sub> is reflected in the increased bond strengths and force constants compared to the pure (6*sσ<sub>g</sub>*) bond in Au<sub>2</sub><sup>-</sup> and Au<sub>2</sub>. The same reasoning accounts for the smaller bond length contraction in going from Pt<sub>2</sub><sup>-</sup> to Pt<sub>2</sub>. The participation of *d*-electrons in the total Pt<sub>2</sub><sup>-</sup> bond strength reduces the relative influence of the 6*sσ<sub>u</sub>*<sup>\*</sup> antibonding electron; so that detachment of a 6*sσ<sub>u</sub>*<sup>\*</sup> electron will not change the bond length for Pt<sub>2</sub><sup>-</sup> as much as for Au<sub>2</sub><sup>-</sup>. The result of this comparison indicates that the participation of the 5*d* electrons in bonding is significant.

A comparison of the palladium and silver dimers is inappropriate because of the different configurations of the *sσ* bonds between both anion and neutral dimers. Comparing Pd<sub>2</sub><sup>-</sup> and Ag<sub>2</sub> would be more appropriate, since each possesses a full (5*sσ<sub>g</sub>*) bond. The bond strengths and force constants of Pd<sub>2</sub><sup>-</sup> and Ag<sub>2</sub> are very similar, which might indicate little *d* electron participation in the Pd<sub>2</sub><sup>-</sup> bond. However, it is difficult to make any definite conclusion regarding *d* bonding in the palladium dimers, because the comparison is between an anionic and a neutral species.

In summary, *d*-electron participation is expected to be more significant in the 4*d* and 5*d* transition metal series because the 5*s* or 6*s* orbitals undergo more contraction than the 4*s* orbital. This effect is especially apparent for the 5*d* series due to relativistic effects. Our experimental results are in good agreement with the theoretical predictions. The relatively small 3*d* orbital in nickel eliminates the possibility of significant *d*-electron bonding. In contrast, the substantial 6*s* orbital contraction in Pt generates large overlap of the 5*d* and 6*s* orbitals, resulting in significant *d*-electron participation in bonding, consistent with Morse's earlier studies.<sup>2</sup>

It is also very interesting to compare our results with other experiments. Previous gas phase experiments have been reported on Ni<sub>2</sub> (Ref. 11) and Pt<sub>2</sub> (Ref. 17) using resonant two-photon ionization spectroscopy. For Ni<sub>2</sub>, the molecular constants, *D*<sub>0</sub>, *r*<sub>e</sub>, and Ω were determined for a low lying electronic state, which was assigned as the ground state. For Pt<sub>2</sub>, only *D*<sub>0</sub> is determined for the ground state. In addition, 26 Pt<sub>2</sub> excited states are detected<sup>17</sup> in the range 11 200–26 300 cm<sup>-1</sup>. Since this region is not accessible to us, comparison between the two exper-

iments is not possible. Recently, Morse<sup>23</sup> has attempted two-photon ionization spectroscopy of Pd<sub>2</sub>. They scanned the spectral region from 11 375 to 23 000 cm<sup>-1</sup> and detected no transitions. They concluded that Pd<sub>2</sub> photoabsorption occurred in their scanning range, but that rapid predissociation prevented Pd<sub>2</sub><sup>+</sup> detection. In comparison, photoelectron spectroscopy provides complementary information concerning the anion ground state and the neutral ground and low-lying electronic states. In particular, we have obtained the anion and neutral vibrational frequencies, the anion geometry, and the anion dissociation energy. These parameters are extremely important for our understanding of the nickel group metal dimers.

## V. CONCLUSION

The negative ion photoelectron spectra of the nickel group metal dimers provide direct information on the electronic ground states and low-lying excited states of the neutral dimers, as well as on the electronic ground states of the anion dimers. The spectra exhibit high densities of low-lying electronic states. The photodetachment transitions are vibrationally resolved for some of the electronic bands. Franck-Condon analyses for these spectra yield spectroscopic constants for the anion ground states and the neutral ground states. The adiabatic electron affinities are determined to be EA(Ni<sub>2</sub>) = 0.926 ± 0.010 eV, EA(Pd<sub>2</sub>) = 1.685 ± 0.008 eV, and EA(Pt<sub>2</sub>) = 1.898 ± 0.008 eV. The dissociation energies of Ni<sub>2</sub><sup>-</sup> and Pt<sub>2</sub><sup>-</sup> are 1.84 ± 0.03 and 2.91 ± 0.03 eV, ~10% smaller than that of the corresponding neutral dimer. The vibrational frequencies of Ni<sub>2</sub><sup>-</sup> and Pt<sub>2</sub><sup>-</sup> are also larger than those of the neutral dimers. D<sub>0</sub>(Pd<sub>2</sub><sup>-</sup>) is found to be 2.15 ± 0.17 eV, more than twice that of the neutral dimer. The comparison of the molecular constants of the nickel group dimers and the coinage metal dimers suggests little 3*d* orbital contribution to the bonding in Ni<sub>2</sub> and Ni<sub>2</sub><sup>-</sup>, but substantial 5*d* contribution in both Pt<sub>2</sub> and Pt<sub>2</sub><sup>-</sup>. This conclusion is consistent with theoretical expectations. For the nickel and platinum dimers, the electronic configurations of the anion and the neutral are *nd*<sup>18</sup>[(*n* + 1)(*sσ<sub>g</sub>*)<sup>2</sup>(*sσ<sub>u</sub>*<sup>\*</sup>)] and *nd*<sup>18</sup>[(*n* + 1)(*sσ<sub>g</sub>*)<sup>2</sup>], *n* = 3 or 5, respectively. For Pd<sub>2</sub><sup>-</sup> and Pd<sub>2</sub>, they are 4*d*<sup>19</sup>(5*sσ<sub>g</sub>*)<sup>2</sup> and 4*d*<sup>19</sup>(5*sσ<sub>g</sub>*)<sup>1</sup>, respectively.

## ACKNOWLEDGMENTS

This research was supported by National Science Foundation Grants Nos. CHE88-19444 and PHY90-12244.

- <sup>1</sup>M. D. Morse, *Chem. Rev.* **86**, 1049 (1986).
- <sup>2</sup>M. D. Morse, in *Advances in Metal and Semiconductor Clusters* (JAI, Greenwich, CT, 1993), Vol. I, p. 83.
- <sup>3</sup>A. B. Anderson, *J. Chem. Phys.* **66**, 5108 (1977).
- <sup>4</sup>J. Harris and R. O. Jones, *J. Chem. Phys.* **70**, 830 (1979).
- <sup>5</sup>T. H. Upton and W. A. Goddard, III, *J. Am. Chem. Soc.* **100**, 5659 (1978); I. Shim, J. Dahl, and H. Johansen, *Int. J. Quantum Chem.* **15**, 311 (1979); J. O. Noell, M. D. Newton, P. J. Hay, R. L. Martin, and F. W. Bobrowicz, *J. Chem. Phys.* **73**, 2360 (1980).
- <sup>6</sup>A. Wolf and H. H. Schmidtke, *Int. J. Quantum Chem.* **18**, 1187 (1980).
- <sup>7</sup>E. M. Spain and M. D. Morse, *J. Chem. Phys.* **97**, 4641 (1992).
- <sup>8</sup>T. C. Devore, A. Ewing, H. F. Franzen, and V. Calder, *Chem. Phys. Lett.* **35**, 78 (1978).
- <sup>9</sup>M. Moskovits and J. E. Hulse, *J. Chem. Phys.* **66**, 3988 (1977).
- <sup>10</sup>F. Ahmed and E. R. Nixon, *J. Chem. Phys.* **72**, 2267 (1979).
- <sup>11</sup>M. D. Morse, G. P. Hansen, P. R. R. Langridge-Smith, L.-S. Zheng, M. E. Geusic, D. L. Michalopoulos, and R. E. Smalley, *J. Chem. Phys.* **80**, 5400 (1984).
- <sup>12</sup>M. D. Morse (private communication).
- <sup>13</sup>H. Basch, D. Cohen, and S. Topoil, *Isr. J. Chem.* **19**, 233 (1980).
- <sup>14</sup>K. Balasubramanian, *J. Chem. Phys.* **87**, 6573 (1987).
- <sup>15</sup>S. K. Gupta, B. M. Nappi, and K. A. Gingerich, *Inorg. Chem.* **20**, 966 (1981).
- <sup>16</sup>K. Jasson and R. Scullman, *J. Mol. Spectrosc.* **61**, 299 (1976).
- <sup>17</sup>S. Taylor, G. W. Lemire, Y. Hamrick, Z.-W. Fu, and M. D. Morse, *J. Chem. Phys.* **89**, 5517 (1988).
- <sup>18</sup>I. Shim and K. Gingerich, *J. Chem. Phys.* **80**, 5107 (1984).
- <sup>19</sup>D. R. Salahub, in *Proceedings of the Nobel Laureate Symposium on Applied Quantum Chemistry*, edited by V. H. Smith, Jr., H. F. Schaeffer III, and K. Morokuma (Deidel, Dordrecht, 1986).
- <sup>20</sup>K. Balasubramanian, *J. Chem. Phys.* **89**, 6310 (1988).
- <sup>21</sup>S. Lee, D. M. Bylander, and L. Kleinman, *Phys. Rev. B* **39**, 4916 (1988).
- <sup>22</sup>S. S. Lin, B. Strauss, and A. Kant, *J. Chem. Phys.* **51**, 2282 (1969).
- <sup>23</sup>S. Taylor, E. M. Spain, and M. D. Morse, *J. Chem. Phys.* **92**, 2710 (1990).
- <sup>24</sup>J. Ho, K. M. Ervin, M. L. Polak, M. K. Gilles, and W. C. Lineberger, *J. Chem. Phys.* **95**, 4845 (1991).
- <sup>25</sup>J. Ho, K. M. Ervin, and W. C. Lineberger, *J. Chem. Phys.* **93**, 6987 (1990); D. G. Leopold, J. Ho, and W. C. Lineberger, *ibid.* **86**, 1715 (1987).
- <sup>26</sup>D. G. Leopold, K. K. Murray, A. E. Stevens, and W. C. Lineberger, *J. Chem. Phys.* **83**, 4849 (1987).
- <sup>27</sup>K. M. Ervin and W. C. Lineberger, in *Advances in Gas Phase Ion Chemistry*, edited by N. G. Adams and L. M. Babcock (JAI, Greenwich, CT, 1992), Vol. 1, pp. 121-166.
- <sup>28</sup>H. Hotop and W. C. Lineberger, *J. Phys. Chem. Ref. Data* **14**, 731 (1985).
- <sup>29</sup>C. E. Moore, *Natl. Bur. Stand. (U.S.) Circ.* **467** (1952).
- <sup>30</sup>K. M. Ervin, J. Ho, and W. C. Lineberger, *J. Chem. Phys.* **91**, 5974 (1989).
- <sup>31</sup>J. L. Hall and M. W. Siegel, *J. Chem. Phys.* **48**, 943 (1968).
- <sup>32</sup>A. Kasdan and W. C. Lineberger, *Phys. Rev. A* **10**, 1658 (1974).
- <sup>33</sup>J. Ho and W. C. Lineberger (unpublished experimental results).
- <sup>34</sup>R. R. Corderman, P. C. Engelking, and W. C. Lineberger, *J. Chem. Phys.* **70**, 4474 (1979); P. C. Engelking and W. C. Lineberger, *Phys. Rev. A* **19**, 149 (1979).
- <sup>35</sup>C. S. Feigerle, Ph.D. thesis, University of Colorado, 1983.
- <sup>36</sup>D. G. Leopold and W. C. Lineberger, *J. Chem. Phys.* **85**, 51 (1986); D. G. Leopold, J. Almöf, W. C. Lineberger, and P. R. Taylor, *ibid.* **88**, 3780 (1987).
- <sup>37</sup>From an *ab initio* calculation by I. Shim, as discussed in Ref. 7.